NANO LETTERS

Letter

pubs.acs.org/NanoLett

On-Chip Single-Plasmon Nanocircuit Driven by a Self-Assembled Quantum Dot

Xiaofei Wu,[†,‡,§,∥] Ping Jiang,[†,⊥] Gary Razinskas,[§,∥] Yongheng Huo,[#] Hongyi Zhang,[‡] Martin Kamp,[∥] Armando Rastelli,[#] Oliver G. Schmidt,[#] Bert Hecht,[§,∥] Klas Lindfors,[*,‡,▽] and Markus Lippitz[*,†,‡]

[†]Experimental Physics III, University of Bayreuth, Universitätsstraße 30, 95447 Bayreuth, Germany

[‡]Max-Planck-Institute for Solid State Research, Heisenbergstraße 1, 70569 Stuttgart, Germany

[§]Experimental Physics V and [∥]Wilhelm Conrad Röntgen Research Center for Complex Material Systems, University of Würzburg, Am Hubland, 97074 Würzburg, Germany

[⊥]College of Science, China University of Petroleum, Changjiang West Road 66, Qingdao 266580, China

[#]Institute for Integrative Nanosciences, IFW Dresden, Helmholtzstraße 20, 01069 Dresden, Germany

[▽]Department of Chemistry, University of Cologne, Luxemburger Straße 116, 50939 Köln, Germany

S *Supporting Information*

ABSTRACT: Quantum photonics holds great promise for future technologies such as secure communication, quantum computation, quantum simulation, and quantum metrology. An outstanding challenge for quantum photonics is to develop scalable miniature circuits that integrate single-photon sources, linear optical components, and detectors on a chip. Plasmonic nanocircuits will play essential roles in such developments. However, for quantum plasmonic circuits, integration of stable, bright, and narrow-band single photon sources in the structure has so far not been reported. Here we present a plasmonic nanocircuit driven by a self-assembled GaAs quantum dot. Through a planar dielectric-plasmonic hybrid waveguide, the quantum dot efficiently excites narrow-band single plasmons that are guided in a two-wire transmission line until they are converted into single photons by an optical antenna. Our work demonstrates the feasibility of fully on-chip plasmonic nanocircuits for quantum optical applications.

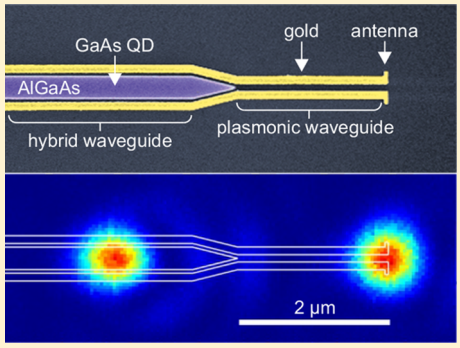

KEYWORDS: *Integrated quantum photonics, quantum plasmonics, single-plasmon, optical nanocircuit, self-assembled quantum dot*

Plasmonic components of photonic circuits feature ultracompact geometries and can be controlled more flexibly and more energy-efficiently compared to conventional dielectric components due to strong field confinement and enhancement.[1,2] Moreover, plasmonic components are compatible with electronic circuits, thanks to their deep subwavelength sizes as well as their electrically conducting materials.[3−5] Therefore, plasmonic nanocircuits have the potential to miniaturize integrated photonic circuits and bridge integrated electronics and photonics.

Recently, the potential of plasmonic nanocircuits also for quantum photonics[6] has been demonstrated. In these works, single emitters such as colloidal nanocrystals and nitrogen vacancy centers in diamond nanocrystals,[7,8] or nonlinear optical processes[9,10] were used as single photon sources. However, the latter require bulky crystals and yield low photon rates, while the former suffer from bleaching, blinking, and poor control of the orientation of the transition dipole moment. Moreover, their emission is also often broadband, and they are not easily excited electrically and are hardly suited for scalable on-chip devices. On the other hand, self-assembled semiconductor quantum dots are stable and nonblinking single photon sources that are electrically drivable and have well-defined orientations of the transition dipole-moments.[11−13] They have been integrated in dielectric on-chip devices by structuring the semiconductor material.[14,15] However, the high refractive index of the semiconductor host material makes it challenging to couple self-assembled quantum dots with surface plasmons, as the conventional way of bringing emitters in the vicinity of plasmonic structures[7,8,16−18] does not work. Here, we address the problem of how to integrate self-assembled semiconductor quantum dots as single-photon sources in plasmonic nanocircuits by releasing the emitters from the bulk crystal and exploiting an indirect-coupling approach.[19]

Our coupling scheme is illustrated in Figure 1a. The structure consists of a bar of AlGaAs heterostructure, which contains a GaAs quantum dot, and a pair of gold wires on both sides of the AlGaAs bar. The structure is placed on a SiO_2 substrate and constitutes an in-plane version of a hybrid waveguide.[20] The

Received: March 27, 2017
Revised: May 30, 2017
Published: June 7, 2017

DOI: 10.1021/acs.nanolett.7b01284
Nano Lett. 2017, 17, 4291−4296

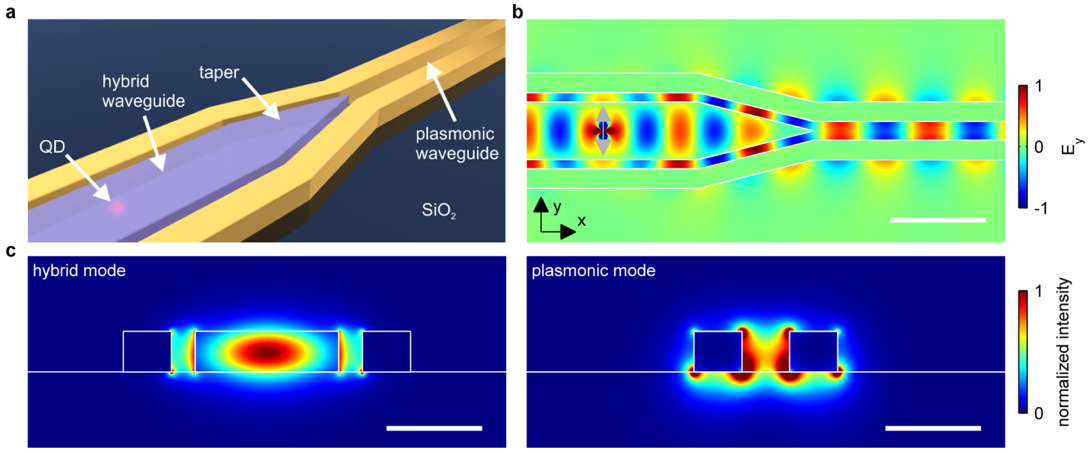

Figure 1. Geometry of the structure and numerically simulated properties. (a) Schematic of the structure for efficient excitation of a plasmonic waveguide with a self-assembled quantum dot. (b) Instant distribution of E_y in the midplane of the structure when excited with a *y*-polarized dipole (light gray arrow) at the center of the waveguide, showing the propagating wave and mode conversion at the taper. The scale bar is 500 nm. (c) Profiles of the relevant modes of the hybrid waveguide (left) and the plasmonic waveguide (right). The electric-field intensity of each panel is normalized in such a way that both modes have the same power. The scale bars are 200 nm. The outlines of the structure are overlaid in (b,c). Detailed dimensions are given in Figure S1 in Supporting Information.

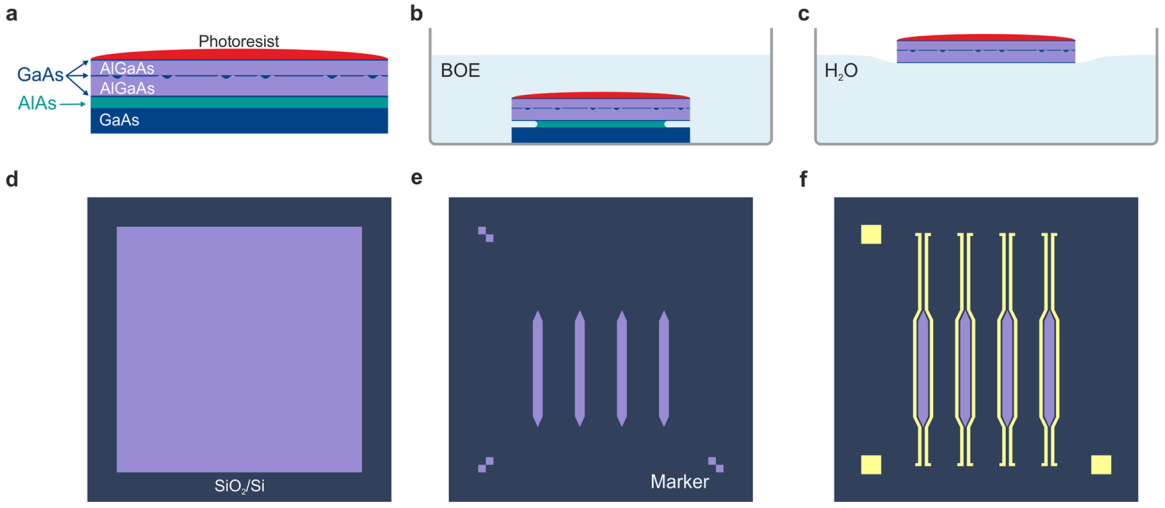

Figure 2. Schematics of sample fabrication (objects not in scale). (a) Structure of the GaAs quantum dot sample (for details see Figure S5 in Supporting Information) with a droplet of resist on top. (b) The sacrificial layer (AlAs) is etched in a BOE solution. (c) The resist and quantum dot membrane are separated from the GaAs substrate by the surface tension of water. (d) The resist and quantum dot membrane are picked up by a new substrate. After the water dries up, the resist is dissolved. (e) The quantum dot membrane is patterned into tapered bars and alignment markers (two touching squares) using EBL and RIE. (f) Gold structures are created and aligned with the semiconductor structures with a second step of EBL and gold deposition.

transition dipole moments of the two energetically almost degenerate bright excitons in the quantum dot are in the plane of the substrate. The hybrid waveguide is transformed into a plasmonic waveguide when the semiconductor bar is tapered, leaving behind only the gold wires. The electromagnetic energy in the hybrid waveguide is thus coupled into surface plasmons propagating along the gold-wire transmission line (Figure 1b).

Numerical analysis reveals that the coupling between the quantum dot and the hybrid waveguide is dominated by the transversal component (*y*-direction in Figure 1b) of the transition dipoles and one of the hybrid waveguide modes (Figure 1c, see also Figures S2−S4 in Supporting Information for details of the modes). In this hybrid mode, the electric field component along the *y*-axis E_y is much stronger than the other two components and is concentrated at the center of the semiconductor. Forty-four percent of the power emitted by a transversal dipole source at the center of the waveguide is transmitted into each propagation direction of the hybrid mode. When the field propagates through the taper, the hybrid mode evolves into a plasmonic mode of the gold-wire transmission line (Figure 1c) with a conversion efficiency of 58%. Taking into account the propagation loss of the hybrid mode, we calculate the plasmon excitation efficiency for the dipole position shown in Figure 1b as 25%. A quantum dot in a bulk, unprocessed crystal, which is used in traditional quantum optical experiments as single-photon source, emits only 2% of its power into free space, and even less is collected by a microscope objective. Our device thus functions as a bright single-plasmon source for on-chip quantum optics. The overall efficiency could be significantly improved by adding a reflector to the hybrid waveguide section to obtain constructive interference in unidirectional propagation.[19,21] This would

DOI: 10.1021/acs.nanolett.7b01284
Nano Lett. 2017, 17, 4291−4296

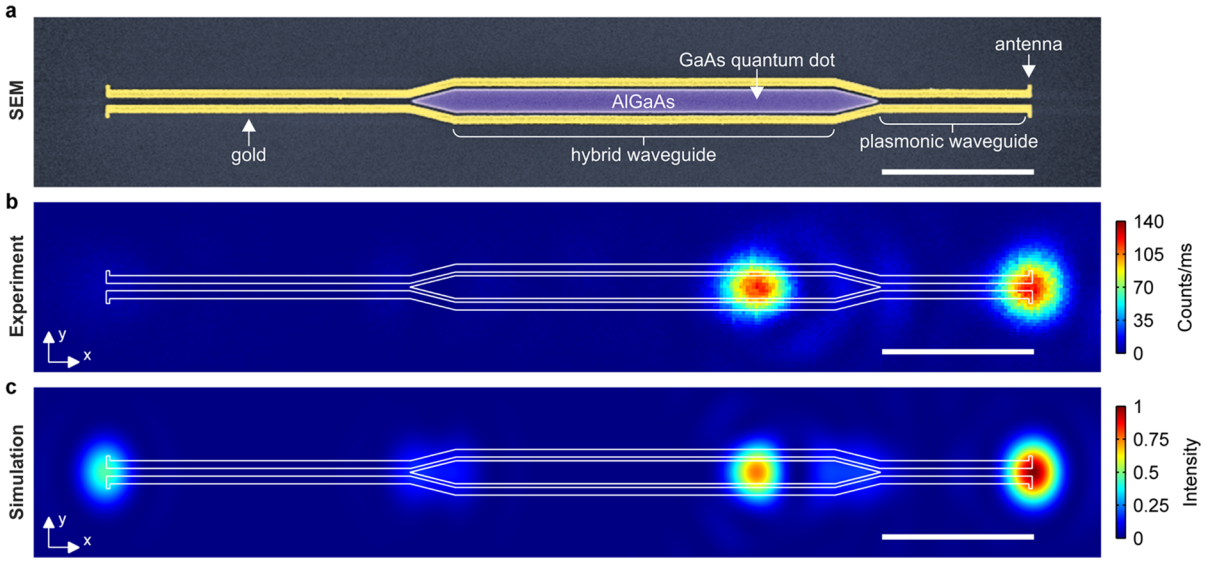

Figure 3. Experimental nanocircuit and observation of efficient plasmon excitation. (a) Scanning electron micrograph of the fabricated structure. A GaAs quantum dot in the AlGaAs bar couples with the hybrid waveguide and excites the plasmonic waveguides through the taper. The plasmons are then guided by the gold-wire transmission lines to the optical antennas. (b) Photoluminescence micrograph of the structure (T = 10 K). The quantum dot is excited by a stationary laser focus. The y-polarized emission is collected by raster-scanning a confocal detection focus. (c) Numerically simulated far-field image following the experimental structure and conditions closely. The excitation source is a pair of incoherent x- and y-polarized dipoles at the quantum dot position of panel (b), and only $|E_y|^2$ in the image plane is plotted. The outlines of the structure are overlaid in (b,c). All scale bars are 2 μm. Detailed dimensions are given in Figure S1 and S5 in Supporting Information.

also result in an increased radiative decay rate of the quantum dot. In the present design, the plasmonic structures do not modify the decay rate of the dot as they are rather far away.

A schematic of the self-assembled quantum dots that are used in our experiments is shown in Figure 2a. These are GaAs quantum dots in AlGaAs barriers grown by molecular beam epitaxy on a GaAs substrate.[22,23] A sacrificial layer (AlAs) is grown in advance on the substrate to enable the separation and thus the transfer of the top quantum dot layers, for which we have developed an epitaxial lift-off approach (Figure 2a–d). Small pieces are cut out of an as-grown quantum dot wafer and then covered with a droplet of a photoresist to protect the quantum dot layers for further processing. The small wafer pieces are immersed in a buffered oxide etch (BOE) solution to etch the AlAs layer. When the etching is finished, the samples are gently taken out of the BOE solution and dipped into ultrapure water with a tweezer. As a result, the resist and the quantum dot layers are separated by the surface tension of water and float on the surface. New substrates are then used to pick up the floating pieces. In the end, the resist is dissolved, leaving the quantum dot membrane on the new substrate. To produce the hybrid structures, the membrane is first patterned into arrays of tapered bars using electron beam lithography (EBL) and reactive ion etch (RIE) (Figure 2e), and gold structures are created and aligned with the semiconductor structures in a second EBL step (Figure 2f).

We choose a simple plasmonic circuit model to prove our idea. A scanning electron micrograph of a fabricated device is shown in Figure 3a. The AlGaAs bar is tapered at both ends and the gold wires are terminated with optical antennas. The optical antennas have been designed to be resonant at the quantum dot emission wavelength of approximately 780 nm with a bandwidth of around 250 nm. When exciting the quantum dot in the AlGaAs bar with a stationary focus of a continuous-wave laser (532 nm wavelength), a raster-scanned confocal detection focus finds bright and stable emission at the position of both the quantum dot and the antenna on the right, shown in Figure 3b for y-polarized emission. Note that the antenna emission is brighter than the direct radiation of the quantum dot, suggesting that plasmons are efficiently launched in the gold-wire transmission line. This experimental result agrees with the simulated far-field image (Figure 3c, see also Figure S6 in Supporting Information). In the simulation, the integrated intensity ratio of the antenna spot to the quantum dot spot is larger than in the experiment. We attribute this disagreement to imperfections of the fabricated structure. Particularly, unexpected loss in the hybrid waveguide is evidenced by additional experimental results (Figure S7 in Supporting Information) and accounts for the dark left antenna in Figure 3b.

To assess the suitability of our plasmon source for quantum optical experiments, we now turn to the spectral and statistical properties of the emitted light. Photoluminescence spectra taken from the spots at the right antenna and the quantum dot of Figure 3b exhibit exactly the same features in terms of the spectral position and width of the sharp lines and their relative intensities (Figure 4a). As these features are a fingerprint for each quantum dot, the spectral correlation shown here further confirms that the quantum dot in the structure is the source of the emission of the antenna. Most importantly, the exciton line is rather narrow for a near-surface quantum dot, although not resolution-limited. We suspect that the sample fabrication has caused broadening of the exciton line, as unprocessed quantum dots show a resolution-limited line width of 60 μeV (see Supporting Information).

To verify that the quantum statistics of the quantum dot emission is preserved by our device and that we really launch single plasmons, we measured the second-order cross-correlation function $g^{(2)}(\tau)$ between the emission in the exciton line collected at the antenna and the quantum dot (Figure 4b). The antibunching dip at time delay τ = 0 goes well below 0.5. The deviation from the ideal value of zero can be fully

DOI: 10.1021/acs.nanolett.7b01284
Nano Lett. 2017, 17, 4291–4296

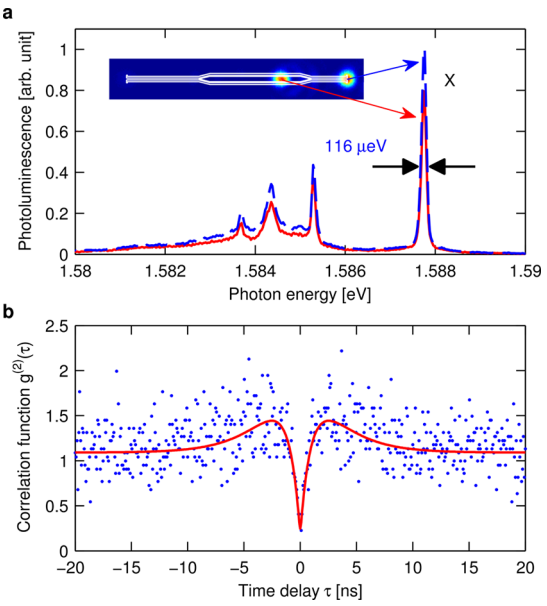

Figure 4. Narrow bandwidth single plasmons. (a) Spectra collected at the position of the quantum dot (red solid line) and antenna at the right end of the structure (blue dashed line). The neutral exciton peaks (X) of both spectra have the same full width at half-maximum of 116 μeV. (b) Measured second-order cross-correlation function $g^{(2)}(\tau)$ between the antenna and quantum dot (blue dots). The red line is a fit to model,[24] taking the off-resonant excitation conditions into account.

explained by the dark-count rate of the detectors and the instrumental response function. This indicates that the quantum dot emits single photons that are coupled into single plasmons in the gold-wire transmission line, and the plasmons are subsequently converted into single photons again by the antenna. At saturated excitation, the detected photon rate is 2 kcps in the exciton line. Taking the detection efficiency of the setup (0.6%) and the simulated collection efficiency (9.5%, defined as the power collected by the objective divided by the power in the plasmonic mode at the taper-end) into account, we estimate a single-plasmon rate of 3×10^6 s^{-1} right after the taper. The ability to efficiently excite and operate with single plasmons provides the basis for quantum applications.

In summary, we have demonstrated a simple model quantum plasmonic nanocircuit with a narrow-band self-assembled GaAs quantum dot as a source for single plasmon excitation. On the basis of our approach, more complex plasmonic as well as photonic circuits can be developed (Figure S8 in Supporting Information). For example, multiple quantum dots can be coupled via plasmonic circuits to achieve photonic transistors.[25] By applying voltages on the gold wires, it may be possible to electrically tune the transitions of the quantum dots into resonance. By using site-controlled self-assembled quantum dots, additional flexibility with device design can be obtained.[14,26] In situ lithography approaches using photoluminescence[27] or cathodoluminescence[28] or approaches of predetermination of the quantum dot position[29] could also help to position quantum dots in devices. Plasmonic components such as interferometers, modulators, and switches[2] can be readily integrated due to the flexible EBL-based fabrication. It is also possible to convert the plasmonic mode in Figure 1c to the other mode of the gold-wire transmission line[30] or to other waveguide modes (e.g., modes on a single gold wire) to fit different purposes. Moreover, electrical excitation of the quantum dot[31,32] and electrical detection of single-plasmons[9,33,34] can be implemented to make all-on-chip circuits.

Semiconductors are well-developed materials for integrated electronic circuits and a wide variety of semiconductor-based quantum photonic circuits are being established as well.[35−37,14] Our work shows that by making use of the self-assembled quantum dots, quantum plasmonic circuits can also be built on semiconductor platforms, and it thus opens the way to integrate electronic, photonic, and plasmonic devices on one semiconductor chip for applications of quantum technologies.

Methods. *Numerical Simulations.* The mode profiles were obtained using a full-vectorial eigenmode solver (MODE Solutions, Lumerical Solutions Inc.). The three-dimensional (3D) electromagnetic simulations of the structures were performed using the finite-difference time-domain method (FDTD Solutions, Lumerical Solutions Inc.). The coupling efficiencies into waveguide modes were calculated by means of a mode expansion analysis, calculating the overlap integrals of the field distribution caused by an emitting dipole in the full 3D structures and the 2D mode profiles.[38] Far-field images were obtained by projection of the simulated near-field intensity distribution recorded 10 nm above the structure into the air half-space taking the numerical aperture (NA) of the collection objective into account. All simulation results are for vacuum wavelength of 780 nm.

Materials and Sample Fabrications. The photoresist used in the epitaxial lift-off approach is NR9-250P from Futurrex, Inc. Before being coated with the resist, the pieces of the quantum dot wafer are cleaned in mild ultrasonic baths of acetone and isopropanol. The samples are baked in an oven at 100 °C for 2 h before the BOE etching. The etching takes place in a solution from BASF (VLSI Selectipur, NH_4F 87.5%) for 10 h. The new substrate is a piece of Si with 400 nm SiO_2. The thickness of SiO_2 is chosen to find a compromise in minimizing charging during EBL, the influence of Si on the optical properties of the waveguide, and having a constructive interference between the direct emission and the reflection of the SiO_2−Si interface. After the water between the membrane and new substrate dries up completely, the resist on the membrane is dissolved by acetone. A 3 nm thick Al_2O_3 layer is deposited on the sample immediately after RIE using atomic layer deposition to protect the semiconductor from oxidation and further processing. The alignment between the semiconductor and gold structures is performed manually using the markers. There is no adhesion layer beneath the gold structures. See Figure S5 in Supporting Information for more details about the sample.

Optical Measurements and Data Processing. A sketch of the optical setup is shown in Figure S9 in Supporting Information. A 532 nm continuous-wave laser diode was used as the excitation source. The laser was focused on the sample by a glass-thickness corrected objective of NA 0.7 through the cryostat window. The sample was cooled down to 10 K. For the confocal luminescence image, a single photon avalanche diode (SPAD) was used to detect the emission in the spectral band of 773−792 nm. A monochromator and a CCD camera were used for acquiring the spectra. The waveguide image was aligned parallel to the grating lines. For the correlation function measurements, the spots of the quantum dot and the antenna were dispersed by the monochromator and only the photons corresponding to the exciton line were transmitted to the two SPADs. The timing output signal of the SPADs were sent to a time-correlated single photon counting unit operating in time-

DOI: 10.1021/acs.nanolett.7b01284
Nano Lett. 2017, 17, 4291−4296

tagged time-resolved mode. The fitting model takes the off-resonant excitation into account[24] (see Supporting Information for more details). The optical characterization results in Figure 3 and 4 are from the same structure. We have determined that the quantum dot investigated here resides exactly at the center of the semiconductor bar in the transversal direction (Figure S10 in Supporting Information), providing an ideal structure for the experiments.

■ ASSOCIATED CONTENT

Supporting Information

The Supporting Information is available free of charge on the ACS Publications website at DOI: 10.1021/acs.nanolett.7b01284.

Detailed dimensions of the designed structure and numerical simulation results; detailed sample fabrication procedure; detailed geometry of real structures and simulation results for real geometry; sketch of the optical setup; additional optical experimental results; sketch of a proposed all-on-chip complex quantum nanocircuit; discussion about the broadening of the exciton line; fitting model of the measured second-order cross-correlation function curve (PDF)

■ AUTHOR INFORMATION

Corresponding Authors

*E-mail (K.L.): klas.lindfors@uni-koeln.de.
*E-mail (M.L.): markus.lippitz@uni-bayreuth.de.

ORCID

Xiaofei Wu: 0000-0002-4594-1678
Klas Lindfors: 0000-0002-6482-5605
Markus Lippitz: 0000-0003-1218-6511

Present Address

(Y.H.) Hefei National Laboratory for Physical Sciences at Microscale and Department of Modern Physics, Shanghai Branch, University of Science and Technology of China, Shanghai 201315, China. (H.Z.) Center for Quantum Information, Institute for Interdisciplinary Information Sciences, Tsinghua University, Beijing 100084, China. (A.R.) Institute of Semiconductor and Solid State Physics, Johannes Kepler University Linz, Altenbergerstraße 69, 4040 Linz, Austria.

Author Contributions

K.L. and M.L. conceived the project. X.W. designed the structures and experiments and constructed the optical setup. Y.H. grew the GaAs quantum dots under supervision of A.R. and O.G.S. X.W. and H.Z. developed the quantum dot membrane transfer method. X.W. and K.L. fabricated the samples. M.K. prepared the transmission electron microscopy lamella and performed the TEM characterization. X.W., P.J., and M.L. carried out the optical measurements and analyzed the data. G.R. performed simulations under supervision of B.H. X.W., K.L., and M.L. wrote the manuscript with input from all authors.

Notes

The authors declare no competing financial interest.

■ ACKNOWLEDGMENTS

We gratefully acknowledge financial support from the Deutsche Forschungsgemeinschaft through SPP1391 Ultrafast Nano-optics (No. LI 1621/3-2). K.L. thanks the University of Cologne for funding through the Institutional Strategy of the University of Cologne within the German Excellence Initiative and the support of the Academy of Finland (Project No. 252421). P.J. acknowledges financial support from the National Natural Science Foundation of China (No. 11204381) and China Scholarship Council. We additionally would like to thank Jürgen Weis and the Nanostructuring Lab team of the Max Planck Institute for Solid State Research for help with sample fabrication and Christian Dicken for help with optical measurements. X.W. thanks Jianjun Chen for valuable discussions.

■ REFERENCES

(1) Sorger, V. J.; Oulton, R. F.; Ma, R.-M.; Zhang, X. Toward Integrated Plasmonic Circuits. *MRS Bull.* **2012**, *37*, 728−738.
(2) *Handbook of Surface Science, Vol. 4: Modern Plasmonics*; Maradudin, A. A., Roy Sambles, J., Barnes, W. L., Eds.; Elsevier: Amsterdam, 2014.
(3) Huang, K. C. Y.; Seo, M.-K.; Sarmiento, T.; Huo, Y.; Harris, J. S.; Brongersma, M. L. Electrically Driven Subwavelength Optical Nanocircuits. *Nat. Photonics* **2014**, *8*, 244−249.
(4) Dionne, J. A.; Sweatlock, L. A.; Sheldon, M. T.; Alivisatos, A. P.; Atwater, H. A. Silicon-Based Plasmonics for On-Chip Photonics. *IEEE J. Sel. Top. Quantum Electron.* **2010**, *16*, 295−306.
(5) Kern, J.; Kullock, R.; Prangsma, J.; Emmerling, M.; Kamp, M.; Hecht, B. Electrically Driven Optical Antennas. *Nat. Photonics* **2015**, *9*, 582−586.
(6) O'Brien, J. L.; Furusawa, A.; Vučković, J. Photonic Quantum Technologies. *Nat. Photonics* **2009**, *3*, 687−695.
(7) de Leon, N. P.; Lukin, M. D.; Park, H. Quantum Plasmonic Circuits. *IEEE J. Sel. Top. Quantum Electron.* **2012**, *18*, 1781−1791.
(8) Huck, A.; Andersen, U. L. Coupling Single Emitters to Quantum Plasmonic Circuits. *Nanophotonics* **2016**, *5*, 483−495.
(9) Heeres, R. W.; Kouwenhoven, L. P.; Zwiller, V. Quantum Interference in Plasmonic Circuits. *Nat. Nanotechnol.* **2013**, *8*, 719−722.
(10) Fakonas, J. S.; Lee, H.; Kelaita, Y. A.; Atwater, H. A. Two-Plasmon Quantum Interference. *Nat. Photonics* **2014**, *8*, 317−320.
(11) Shields, A. J. Semiconductor Quantum Light Sources. *Nat. Photonics* **2007**, *1*, 215−223.
(12) Gazzano, O.; Almeida, M. P.; Nowak, A. K.; Portalupi, S. L.; Lemaître, A.; Sagnes, I.; White, A. G.; Senellart, P. Entangling Quantum-Logic Gate Operated with an Ultrabright Semiconductor Single-Photon Source. *Phys. Rev. Lett.* **2013**, *110*, 250501.
(13) Müller, M.; Bounouar, S.; Jöns, K. D.; Glässl, M.; Michler, P. On-Demand Generation of Indistinguishable Polarization-Entangled Photon Pairs. *Nat. Photonics* **2014**, *8*, 224−228.
(14) Dietrich, C. P.; Fiore, A.; Thompson, M. G.; Kamp, M.; Höfling, S. GaAs Integrated Quantum Photonics: Towards Compact and Multi-Functional Quantum Photonic Integrated Circuits. *Laser Photon. Rev.* **2016**, *10*, 870−894.
(15) Lodahl, P.; Mahmoodian, S.; Stobbe, S. Interfacing Single Photons and Single Quantum Dots with Photonic Nanostructures. *Rev. Mod. Phys.* **2015**, *87*, 347−400.
(16) Lee, H. S.; Kim, M. S.; Jin, Y.; Han, G. H.; Lee, Y. H.; Kim, J. Efficient Exciton−Plasmon Conversion in Ag Nanowire/Monolayer MoS_2 Hybrids: Direct Imaging and Quantitative Estimation of Plasmon Coupling and Propagation. *Adv. Opt. Mater.* **2015**, *3*, 943−947.
(17) de Torres, J.; Ferrand, P.; Colas des Francs, G.; Wenger, J. Coupling Emitters and Silver Nanowires to Achieve Long-Range Plasmon-Mediated Fluorescence Energy Transfer. *ACS Nano* **2016**, *10*, 3968−3976.
(18) Weeber, J.-C.; Hammani, K.; Colas-des-Francs, G.; Bouhelier, A.; Arocas, J.; Kumar, A.; Eloi, F.; Buil, S.; Quélin, X.; Hermier, J.-P.; et al. Colloidal Quantum Dot Integrated Light Sources for Plasmon Mediated Photonic Waveguide Excitation. *ACS Photonics* **2016**, *3*, 844−852.

DOI: 10.1021/acs.nanolett.7b01284
Nano Lett. 2017, 17, 4291−4296

(19) Davanco, M.; Liu, J.; Sapienza, L.; Zhang, C.-Z.; Cardoso, J. V. D. M.; Verma, V.; Mirin, R.; Nam, S. W.; Liu, L.; Srinivasan, K. A Heterogeneous III-V/Silicon Integration Platform for on-Chip Quantum Photonic Circuits with Single Quantum Dot Devices. 2016, arXiv:1611.07654. arXiv.org e-Print archive. https://arxiv.org/abs/1611.07654 (accessed May 08, 2017).
(20) Oulton, R. F.; Sorger, V. J.; Genov, D. A.; Pile, D. F. P.; Zhang, X. A Hybrid Plasmonic Waveguide for Subwavelength Confinement and Long-Range Propagation. *Nat. Photonics* **2008**, *2*, 496−500.
(21) Fu, A.; Gao, H.; Petrov, P.; Yang, P. Widely Tunable Distributed Bragg Reflectors Integrated into Nanowire Waveguides. *Nano Lett.* **2015**, *15*, 6909−6913.
(22) Huo, Y. H.; Witek, B. J.; Kumar, S.; Cardenas, J. R.; Zhang, J. X.; Akopian, N.; Singh, R.; Zallo, E.; Grifone, R.; Kriegner, D.; et al. A Light-Hole Exciton in a Quantum Dot. *Nat. Phys.* **2014**, *10*, 46−51.
(23) Zhang, H.; Huo, Y.; Lindfors, K.; Chen, Y.; Schmidt, O. G.; Rastelli, A.; Lippitz, M. Narrow-Line Self-Assembled GaAs Quantum Dots for Plasmonics. *Appl. Phys. Lett.* **2015**, *106*, 101110.
(24) Regelman, D.; Mizrahi, U.; Gershoni, D.; Ehrenfreund, E.; Schoenfeld, W.; Petroff, P. Semiconductor Quantum Dot: A Quantum Light Source of Multicolor Photons with Tunable Statistics. *Phys. Rev. Lett.* **2001**, *87*, 257401.
(25) Chang, D. E.; Sørensen, A. S.; Demler, E. A.; Lukin, M. D. A Single-Photon Transistor Using Nanoscale Surface Plasmons. *Nat. Phys.* **2007**, *3*, 807−812.
(26) Jöns, K. D.; Atkinson, P.; Müller, M.; Heldmaier, M.; Ulrich, S. M.; Schmidt, O. G.; Michler, P. Triggered Indistinguishable Single Photons with Narrow Line Widths from Site-Controlled Quantum Dots. *Nano Lett.* **2013**, *13*, 126−130.
(27) Dousse, A.; Lanco, L.; Suffczyński, J.; Semenova, E.; Miard, A.; Lemaître, A.; Sagnes, I.; Roblin, C.; Bloch, J.; Senellart, P. Controlled Light-Matter Coupling for a Single Quantum Dot Embedded in a Pillar Microcavity Using Far-Field Optical Lithography. *Phys. Rev. Lett.* **2008**, *101*, 267404.
(28) Gschrey, M.; Thoma, A.; Schnauber, P.; Seifried, M.; Schmidt, R.; Wohlfeil, B.; Krüger, L.; Schulze, J.-H.; Heindel, T.; Burger, S.; et al. Highly Indistinguishable Photons from Deterministic Quantum-Dot Microlenses Utilizing Three-Dimensional in Situ Electron-Beam Lithography. *Nat. Commun.* **2015**, *6*, 7662.
(29) Pfeiffer, M.; Lindfors, K.; Zhang, H.; Fenk, B.; Phillipp, F.; Atkinson, P.; Rastelli, A.; Schmidt, O. G.; Giessen, H.; Lippitz, M. Eleven Nanometer Alignment Precision of a Plasmonic Nanoantenna with a Self-Assembled GaAs Quantum Dot. *Nano Lett.* **2014**, *14*, 197−201.
(30) Dai, W.-H.; Lin, F.-C.; Huang, C.-B.; Huang, J.-S. Mode Conversion in High-Definition Plasmonic Optical Nanocircuits. *Nano Lett.* **2014**, *14*, 3881−3886.
(31) Yuan, Z.; Kardynal, B. E.; Stevenson, R. M.; Shields, A. J.; Lobo, C. J.; Cooper, K.; Beattie, N. S.; Ritchie, D. A.; Pepper, M. Electrically Driven Single-Photon Source. *Science* **2002**, *295*, 102−105.
(32) Bennett, A. J.; Unitt, D. C.; See, P.; Shields, A. J.; Atkinson, P.; Cooper, K.; Ritchie, D. A. Microcavity Single-Photon-Emitting Diode. *Appl. Phys. Lett.* **2005**, *86*, 181102.
(33) Heeres, R. W.; Dorenbos, S. N.; Koene, B.; Solomon, G. S.; Kouwenhoven, L. P.; Zwiller, V. On-Chip Single Plasmon Detection. *Nano Lett.* **2010**, *10*, 661−664.
(34) Falk, A. L.; Koppens, F. H. L.; Yu, C. L.; Kang, K.; de Leon Snapp, N.; Akimov, A. V.; Jo, M.-H.; Lukin, M. D.; Park, H. Near-Field Electrical Detection of Optical Plasmons and Single-Plasmon Sources. *Nat. Phys.* **2009**, *5*, 475−479.
(35) Bogdanov, S.; Shalaginov, M. Y.; Boltasseva, A.; Shalaev, V. M. Material Platforms for Integrated Quantum Photonics. *Opt. Mater. Express* **2017**, *7*, 111−132.
(36) Bettotti, P. Hybrid Materials for Integrated Photonics. *Adv. Opt.* **2014**, *2014*, 891395.
(37) Silverstone, J. W.; Bonneau, D.; O'Brien, J. L.; Thompson, M. G. Silicon Quantum Photonics. *IEEE J. Sel. Top. Quantum Electron.* **2016**, *22*, 390−402.
(38) Snyder, A. W.; Love, J. D. Fundamental Properties of Modes. *Optical Waveguide Theory*; Chapman and Hall: London, 1983.

DOI: 10.1021/acs.nanolett.7b01284
Nano Lett. 2017, 17, 4291−4296